NeuroImage 197 (2019): 295 – 305

DOI: https://doi.org/10.1016/j.neuroimage.2019.04.066

Oscillatory brain mechanisms supporting response cancellation in selective stopping strategies

Alberto J. Sánchez-Carmona[1*], Gerardo Santaniello[1,2], Almudena Capilla[3], José Antonio Hinojosa[1, 4], Jacobo Albert[1, 3*]

[1]Instituto Pluridisciplinar, Universidad Complutense de Madrid, 28040 Madrid, Spain

[2]Departamento de Medicina y Cirugía, Psicología, Medicina Preventiva y Salud Pública Inmunología y Microbiología Médica, Enfermería y Estomatología, Universidad Rey Juan Carlos, Spain.

[3]Facultad de Psicología, Universidad Autónoma de Madrid, 28049 Madrid, Spain

[4]Facultad de Psicología, Universidad Complutense de Madrid, 28223, Madrid, Spain

***Corresponding authors**: A.J. Sánchez-Carmona. Instituto Pluridisciplinar, Universidad Complutense de Madrid, Paseo Juan XXIII, nº1, 28040 Madrid, Spain. E-mail: albertosanchezcarmona@gmail.com; J. Albert. Facultad de Psicología. Universidad Autónoma de Madrid, 28049 Madrid, Spain. E-mail: jacobo.albert@uam.es.

Abbreviated title: Oscillatory brain activity during selective stopping strategies

Abstract

Although considerable progress has been made in understanding the neural substrates of simple or global stopping, the neural mechanisms supporting selective stopping remain less understood. The selectivity of the stop process is often required in our everyday life in situations where responses must be suppressed to certain signals but not others. Here, we examined the oscillatory brain mechanisms of response cancellation in selective stopping by controlling for the different strategies adopted by participants (n=54) to accomplish a stimulus selective stop-signal task. We found that successfully cancelling an initiated response was specifically associated with increased oscillatory activity in the high-beta frequency range in the strategy characterized by stopping selectively (the so called *dependent Discriminate then Stop, dDtS*), but not in the strategy characterized by stopping non-selectively *(Stop then Discriminate, StD*). Beamforming source reconstruction suggests that this high-beta activity was mainly generated in the superior frontal gyrus (including the pre-supplementary motor area) and the middle frontal gyrus. Present findings provide neural support for the existence of different strategies for solving selective stopping tasks. Specifically, differences between strategies were observed in the oscillatory activity associated with the stop process and were restricted to the high-beta frequency range. Moreover, current results provide important evidence suggesting that high-beta oscillations in superior and middle frontal cortices play an essential role in cancelling an initiated motor response.

Keywords: selective stopping; brain oscillations; high beta frequency band; pre-SMA; response cancellation.

1. Introduction

The ability to interrupt unwanted thoughts and actions is a hallmark of goal-directed behavior. Research on the neural bases of response inhibition has mainly focused on simple or global stopping, in which all responses should be inhibited when the stop signal occurs. However, in everyday life, individuals must often inhibit certain responses but not others (response-selective stopping), or responses to certain signals but not others (stimulus-selective stopping). Here, we examined the oscillatory brain activity of stimulus selective stopping.

Prior research has shown that participants use different strategies in stimulus-selective stop signal tasks (Bissett & Logan, 2014). In this paradigm, participants are asked to respond as quickly as possible to repeated presentations of a stimulus (go trial), cancel their already initiated response when presented with a second, infrequent signal (stop trial), but continue responding if another infrequent signal is presented (continue or ignore trial). However, whereas some participants selectively interrupt their responses to stop signals (*Discriminate then Stop strategy -DtS-* strategy), other participants withhold their responses whenever a signal occurs (either ignore or stop), and thereafter restart the cancelled response if an ignore signal was presented (*Stop then Discriminate -StD-* strategy). Moreover, the *DtS* strategy can be further divided into dependent (*dDtS*) and independent (*iDtS*), depending on whether the independence assumption of the horse-race model used to calculate the stop-signal reaction time (SSRT) is violated or not (Bissett & Logan, 2014; Logan, 1994; Verbruggen & Logan, 2009). This model posits that response inhibition is the outcome of a race between the go and the stop process. If the go process finishes the race before the stop process, individuals will fail to inhibit their response. By contrast, if the stop process ends before the go process, the response will be inhibited. Importantly, the model assumes that go

and stop processes are contextually independent (Bissett & Logan, 2014; Logan, 1994; Verbruggen & Logan, 2009). This assumption enables to predict that failed-stop responses (commission errors) should be shorter than correct go responses, given that failed-stop trials indeed reflect that going processes finished the race before stopping processes. Of note, the independence assumption between the stop and the go process is met in the *StD* strategy, but not in all individuals using the *DtS* strategy (Bisset & Logan, 2014). In those adopting the *dDtS* strategy, RTs in failed-stop trials are not shorter than RTs in correct go trials. This is thought to be due to the emergence of dependence between going and discriminating (stop vs. ignore) processes in this strategy. The violation of the independence assumption has important implications for the calculation of the SSRT (see Verbruggen & Logan, 2009). Thus, it has been recommended to use the ignore RT distribution rather than the go RT distribution to estimate the latency of the stop process (SSRT) in the *dDtS* strategy (Bisset & Logan, 2014). It is worth mentioning that this solution might be valid only under some assumptions that have not been fully tested.

To our knowledge, only two prior studies have compared the brain activity associated with each of these main strategies used in stimulus-selective stop tasks. In an event-related potentials (ERP) study using source localization methods, Sanchez-Carmona and colleagues (2016) found no differences in electrophysiological activity between stop and ignore conditions around the latency that was estimated for the stop process (i.e., the end of the SSRT) in the *StD* strategy. By contrast, differences between these two conditions were evident around the end of the SSRT for those individuals who used a strategy in which the response interruption process was selective to stop signal (*dDtS*). Specifically, they found increased P3 amplitudes and prefrontal activity for the stop versus ignore condition. These findings were in line with the behavioral-

based strategy classification made by Bisset and Logan (2014), and provided new evidence suggesting that the P3 onset and its neural generators (including, inferior, medial and middle frontal gyri) may be a reliable neural marker of response cancellation process. Similarly, a recent fMRI study has also provided evidence for distinct brain activity patterns supporting selective and non-selective strategies, but differences were mainly observed in a processing stage prior to response interruption process (Sebastian, et al., 2017).

The goal of the present study was to further characterize the neural mechanisms of stimulus-selective stopping strategies by examining the oscillatory neuronal activation associated with the cancellation of the ongoing response in each strategy using scalp and source-level time-frequency measures. To this end, we compared activation patterns elicited by successful stop versus successful ignore signals. This functional comparison has been recommended over traditional contrasts (successful stop vs. successful go, failed stop vs. successful stop) for isolating the neural substrates specifically underlying response cancellation, because it minimizes the influence of confounding factors such as attentional capture, conflict monitoring, and emotional frustration (Etchell, Sowman, & Johnson, 2012; Li, Huang, Constable, & Sinha, 2006; Sánchez-Carmona, Albert, & Hinojosa, 2016; Sharp, et al., 2010).

Time-frequency analysis of EEG data are expected to provide useful information beyond that coming from ERP-based analyses, because they both capture different aspects of neural activity (Cohen, 2014). For instance, a remarkable amount of information from EEG recordings might be only observed in time-frequency-based analyses if that information is non-phase-locked to stimuli (Cohen, 2014). Moreover, time-frequency data analyses allow inferences regarding neural oscillations. In this sense, it has recently been proposed that oscillatory dynamics might play a critical role

in global stopping (Aron, Herz, Brown, Forstmann, & Zaghloul, 2016; Lavallee, Meemken, Herrmann, & Huster, 2014). Specifically, it has been argued that the global stopping-related network, which comprises prefrontal cortex (primarily, inferior frontal gyrus -IFG- and pre-supplementary motor cortex -pre-SMA- and subthalamic nucleus -STN-: (Chikazoe, Konishi, Asari, Jimura, & Miyashita, 2007; Li, et al., 2006; Li, Yan, Sinha, & Lee, 2008), might operate via communication in the beta frequency band (Aron, et al., 2016; Wagner, Wessel, Ghahremani, & Aron, 2018). Theta-band activity has also been associated with stopping (Isabella, Ferrari, Jobst, Cheyne, & Cheyne, 2015; Jha, et al., 2015; Nigbur, Ivanova, & Stürmer, 2011), although it is not clear yet whether activity within this band indexes the response cancellation process, or rather reflects a general marker for executive control or conflict monitoring (Cavanagh & Frank, 2014; Nigbur, et al., 2011). It should be noted that many of the studies that examined the role of theta oscillations in response cancellation, also manipulated task complexity at either stimuli or response selection levels (Isabella, et al., 2015; Jha, et al., 2015; Wessel & Aron, 2014). This could have introduced a bias in favour of a prominent role of theta-band oscillations in response inhibition. In any case, this previous evidence mainly relies on successful stop versus failed stop comparison, while the successful stop versus ignore contrast has been little explored. Thus, the results of the present study may also shed light on the identification of the neural oscillations specifically involved in response cancellation. Additionally, although gamma-band activity has not been directly related to response cancellation, prior evidence suggests its involvement in several processes associated with stop-signal tasks such as proactive inhibition (“preparation to stop”, Swan et al., 2012; Swan et al., 2013), the processing of the contextual complexity of the task (Jha, et al., 2015), and the monitoring that occurs

during the selection of the correct movement (Isabella, Ferrari, Jobst, Cheyne, Cheyne, 2015).

The relationship between beta and theta oscillations and the different strategies used in selective stopping tasks remains unexplored. Based on prior literature (Aron, et al., 2016; Wagner, Wessel, Ghahremani, & Aron, 2018; Bisset & Logan, 2014), we hypothesize that increased beta band activity at scalp and source level will be observe during the cancellation of the ongoing response in selective (*DtS*) but not in non-selective (*StD*) stopping strategies. These findings would provide additional support for the existence of different strategies to cope with the demands involved in stimulus-selective stopping tasks (Bissett & Logan, 2014). Additionally, they would argue in favor of a critical involvement of beta oscillations in the cancelation of an initiated response. Regarding theta activity, we would expect the same pattern of results only if we assume that theta-band oscillations reflect the response cancellation process rather than executive control or conflict monitoring. Finally, given prior findings suggesting a role of gamma activity in several general aspects of stop-signal tasks, we also examined activity in this frequency band. However, since no prior study specifically associated gamma activity with response cancellation, no hypotheses could be outlined here.

2. Materials and Methods

2.1. Participants

Sixty-five right-handed graduate and undergraduate students (mean age=20.9; SD=1.41) participated in this experiment. The study was approved by the local ethics committee, and informed consent was obtained from each subject prior to the experiment. All participants reported normal or corrected-to-normal visual acuity and had no history of neurological or psychiatric disorders. Eleven subjects were excluded from the analyses,

three of them due to low overall task accuracy (more than 25 errors, <2.5 SDs below the group mean), two of them due to unusual slow go RTs (more than 970 ms, >2.5 SDs above the group mean), and four of them due to non-linear adjustment of their inhibition functions (see Sanchez-Carmona 2016 for more details of this exclusion criterion). Briefly, if task instructions were fulfilled, the probability to respond given the stop signal (failed inhibition) should increment monotonically from 0 to 1 as stop signal delay (SSD) values increases (Verbruggen & Logan, 2009): stopping the ongoing response is easier if the stop signal is presented far in advance of the completion of the go response, and more difficult if the stop signal is presented closer to the completion of the go response. Therefore, non-linear adjustment of a subject's inhibition function indicates that the participant did not perform the task following task instructions (i.e., responding as soon as possible when the go stimulus was presented). Thus, the final sample consisted of 54 participants. All of them met the binomial stop-signal distribution criterion, reporting a 0.5 probability of stopping the ongoing response. Subsequently, participants were divided according to the strategy used to perform the experimental task. The results of the analyses indicated that 33 subjects employed the *StD* strategy, whereas 21 subjects used the *dDtS* strategy. Any subject was identified under *iDts* strategy. The resulting two groups were matched for age ($t(52)=0.97$, $p=0.33$) and gender ($\chi^2 =0.56$, $p=0.45$).

2.2. Experimental Design

Participants performed a stimulus-selective stop signal task (see Sánchez-Carmona et al., 2016 for details) with three different stimuli: go, stop and ignore (Figure 1). These stimuli were three geometrical shapes colored in white against a black background (an arrow, a square and a diamond). Subjects were instructed to press either the left or the

right key arrows in a keyboard with their respective index finger whenever an arrow pointing to any of these two orientations was presented (go trial). In addition, they were informed that in some trials they had to stop their response when seeing a square surrounding the arrow (stop trial), but to continue responding if a diamond was presented around the arrow (ignore trial). Critically, we insisted participants to respond as fast and accurate as possible on go and ignore trials, and as accurate as possible on stop trials, trying to interrupt their ongoing responses. Subjects were instructed not to wait for the square or diamond to appear. Otherwise, the assumptions in which task parameter estimations were based would be compromised (Verbruggen, Chambers, & Logan, 2013). These instructions were presented to the participants on the computer monitor at the beginning of the experiment. Also, task instructions were verbally reminded to participants between blocks.

*** Figure 1 around here***

The whole task consisted of 1000 trials grouped into four blocks, each containing 250 trials (150 go, 50 stop and 50 ignore). This number of trials was based on a priori power analysis (G*Power 3.1, (Faul, Erdfelder, Buchner, & Lang, 2009). Each trial began with a black screen with a random duration between 500 and 1000 ms. Thereafter, a go stimulus was presented. Arrows randomly pointed to the left or to the right in half of the trials. In 20% of the trials (50 trials per block), the stop signal was presented after a variable delay (SSD). This delay was initially set at 200 ms and was dynamically adjusted from stop trial to stop trial according to the individual performance of each participant. After a successful inhibition, the SSD was increased (+50 ms), which gave some advantage to the go process and reduced the probability of a

successful inhibition in the next stop trial. If a response was emitted in the last stop trial, the SSD decreased (-50 ms), so the stop process started earlier and the probability of a response interruption in the next stop trial increased. This staircase algorithm was applied to achieve 0.5 probability of responding to a stop signal (Levitt, 1971). In another 20% of the trials (50 trials per block), the ignore stimulus was presented after the go stimulus. The delay was also initially fixed to 200 ms, but importantly, the ignore signal delay (ISD) was equated to the most recent SSD. Thus, the adaptive adjustment of SSD was never applied after an ignore trial. In the remaining trials (60%), only go stimuli were presented (150 trials per block).

Participants carried out the experimental task seated comfortably in an electrically shielded and sound-attenuated room. Task stimuli were presented on a computer monitor that was positioned at eye level about 65 cm in front of the participant. The stimuli were displayed on a 19-inch LCD-LED Samsung 943 N color monitor with a 75-Hz refresh rate, a 5:4 aspect ratio, and a resolution of 1024×768. Before the beginning of the experimental blocks, subjects completed a practice block of 100 trials to ensure that they understood task instructions (60 go, 20 stop and 20 ignore trials; initial SSD=200 ms). The task was designed and implemented in MATLAB, using Psychtoolbox (www.psychtoolbox.org). The Matlab script of stop-it (Verbruggen, Logan, & Stevens, 2008) served as starting point for programming our stimulus-selective stop-signal task.

2.3. EEG recording

Electroencephalogram (EEG) activity was recorded from 62 electrode locations mounted in an electrode cap (BrainVision), arranged according to the International 10–

10 system (American Electroencephalographic Society, 1991). All electrodes were referenced to the average of mastoids. Bipolar horizontal and vertical electrooculograms (EOGs) were also recorded to monitor eye movements and blinks. Electrode impedances were kept below 10 kΩ. Recordings were amplified using BrainAmp amplifiers (BrainProducts, Munich, Germany), continuously digitized at a sample rate of 1000 Hz, and filtered online with a frequency band-pass of 0.01–100 Hz.

2.4. Data Analysis

2.4.1. Behavioural analysis

Each subject's strategy was determined by comparing their mean no-signal (go) RT, stop-respond RT (incorrectly executed responses on stop-signal trials) and ignore RT (correctly executed response on ignore-signal trials), following the procedure described by Bisset and Logan (2014). Participants were categorically [1]classified as using the *iDtS* strategy (stop-respond RT<no-signal RT ≮ignore RT), *StD* strategy (stop-respond RT<no-signal RT<ignore RT) or *dDtS* strategy (stop-respond RT≮no-signal RT<ignore RT). Bayes Factor was used to compare the evidence for and against the null hypotheses without bias (Rouder, Speckman, Sun, Morey, & Iverson, 2009). The Bayes factor is a ratio that contrasts the likelihood of the data fitting under the null hypothesis with the likelihood of fitting under the alternative hypothesis. A Bayes factor of 1 means that the odds in favor of the null hypothesis are no better than the odds against it. Bayes factor was computed by calculating the mean and standard deviations of no-signal, stop-respond, and ignore RTs separately for each subject. Subsequently, we calculated two

[1] Participants were also dimensionally classified in a 2D space using go and failed stop reaction times (RT) in order to examine whether the individual difference on the *StD-DtS* dimension correlate with neural oscillatory features. A detailed description of this dimensional approach to selective stopping strategies and the correlational analysis with oscillatory measures can be found in the Supplementary Material.

independent samples t tests comparing stop-respond RT with no-signal RT and ignore RT with no-signal RT, respectively. Rouder's Bayes factor calculator on the Perception and Cognition Lab website (http://pcl.missouri.edu/bf-two-sample) was used to convert t tests and sample sizes to Bayes factors. The recommended Jeffrey-Zellner-Slow Prior with the default value of 1 was used, which is appropriate if there are no strong prior assumptions (Rouder, et al., 2009). SSRTs were computed via the integration method since it has been shown to be less biased than the traditional mean method when the normality criterion in the go RT distribution is violated (Verbruggen, et al., 2013). We computed SSRTs over both go and ignore RT distributions, as recommended by Bisset and Logan (2014) when dealing with these strategies. Notably, the independence assumption made by the horse race model is violated in the dDtS strategy, so calculating SSRT using the go RT distribution as the underlying go distribution on stop trials is an invalid method. As Bisset and Logan (2014) have suggested, a possible solution to this problem is to use the ignore RT distribution to calculate SSRT in this strategy. However, it is worth mentioning that that this procedure might be valid only under some assumptions that have not been yet tested. Therefore, SSRTs computed using the ignore RT distribution for the subjects who adopted the dDtS strategy should be interpreted with caution until being validated.

2.4.2. Preprocesing and time-frequency analysis

Data were analyzed using Fieldtrip package (http://www.fieldtriptoolbox.org; (Oostenveld, Fries, Maris, & Schoffelen, 2011) for MATLAB (Mathworks, Inc.). EEG activity was first down-sampled to 500 Hz to save calculation time and memory costs. The continuous EEG was then segmented into epochs time-locked to stop/ignore signal onset. The duration of the epochs was 1900 ms (from -700 to +1200 ms). However, to

overcome problems arising from the choice of the baseline period just prior to stop/ignore onset (some epochs but not others may contain activity related to go processing), we rather employed the time interval between 400 and 200 ms before go stimulus onset as baseline (during this period, participants saw a black screen -inter-trial interval-). Analyses were focused on stop and ignore trials to maximize the control of confounding variables that are not related to response cancellation (Albert, López-Martín, Hinojosa, & Carretié, 2013; Etchell, et al., 2012; Sánchez-Carmona, et al., 2016; Sharp, et al., 2010). Importantly, ignore trials in which subjects did not press any key or pressed a wrong key of the keyboard, as well as stop trials in which subjects responded to stop stimulus were discarded. Likewise, we also discarded stop and ignore trials where a response was emitted before signal presentation. Independent component analysis (ICA) was then used to remove ocular and other artifacts from individual EEG data sets (Jung, et al., 2000). After the ICA-based removing process, visual inspection of individual EEG epochs was also conducted to remove residual artifacts. The artifact rejection and exclusion of incorrect or miss trials, led to the average admission of 148.9 (18.89) ignore trials and 77.8 (10.03) stop trials.

To obtain a time-frequency representation of each single trial, we applied the short-time Fast Fourier Transform (FFT) with a Hanning tapper. The FFT was performed on overlapping 400-ms windows in 950 steps. Such length was selected to capture at least one cycle of the minimum frequency aimed to study (i.e., theta band activity). Given the frequency resolution provided by the selected time segment and the sampling rate used, we selected the closest frequency bin to a frequency comprised between 2.5 and 50 Hz in a logarithmic scale. Thus, the resulting power at each time point and frequency bin was consecutively placed into a time-frequency space for each trial and participant,

from -500 to +1000 after stop/ignore stimulus. Before statistical analyses, the resulted power was normalized by taking a decibel transformation relative to baseline (dB_{tf} =10log10[$activity_{tf}$ - mean ($baseline_f$)]).

2.4.3. Statistical analysis at scalp level

We focused on theta (4-7 Hz), beta (12-30 Hz) and gamma (31-50 Hz) bands oscillations because they have been proposed to play important roles in stopping (Aron, et al., 2016; Huster, Enriquez-Geppert, Lavallee, Falkenstein, & Herrmann, 2013; Isabella, et al., 2015; Jha, et al., 2015; N. Swann, et al., 2009; N. C. Swann, et al., 2012). Following previous studies (Lavallee, et al., 2014; Marco-Pallarés, Camara, Münte, & Rodríguez-Fornells, 2008; Ritter, Moosmann, & Villringer, 2009; N. Swann, et al., 2009; Wagner, et al., 2018), beta band was divided into lower (12-20 Hz) and upper subbands (21-30 Hz). Therefore, mean theta (4-7 Hz), low-beta (12–20 Hz), high-beta (21–30 Hz) and gamma (31-50 Hz) values were extracted between 100 ms to 700 ms post-stop and ignore stimulus, thus comprising enough time to include SSRT latency. Importantly, due to the logarithmic scale employed in the time-frequency analysis, each average included an equivalent number of frequency bins, thus avoiding the overrepresentation of higher frequencies. So that, taking advantage of the high temporal resolution of EEG, we aimed to fully explore when and where power changes are induced by each signal type (stop and ignore) with minimal a priori assumption.

To handle the multiple comparison problem, we performed cluster-based nonparametric permutation tests. Under the null hypothesis of exchangeability, marginal distributions of stop and ignore conditions are equal, so relative power observed in them can be shuffled. Thus, time-channel samples were highlighted as significant if their value exceeds the 97.5th percentile or do not surpass the 2.5th percentile (statistical

346 threshold at p=0.05 for a two-sided test) of an empirical null hypothesis distribution
347 computed in the following way: in every shuffle, a paired two-sided t-test was
348 performed between each time-channel sample, setting up the pre-cluster threshold at
349 p<0.05. However, given the autocorrelation in the data, a finding was considered
350 significant only if enough neighbouring samples were also significant (spatio-temporal
351 contiguity criterion). After each iteration, statistical maps of suprathreshold and
352 infrathreshold clusters were conformed, and only the largest and the smallest sum of test
353 statistics within them were stored, controlling the multiple comparison problem. This
354 procedure was repeated 1000 times to build a distribution of the largest suprathreshold
355 and the smallest infrathreshold clusters that can be expected under the null hypothesis.
356 All permutation statistics were done using FieldTrip.
357
358 *2.4.4. Source reconstruction*
359 To estimate the neural sources underlying the experimental effects observed at scalp
360 level, a time domain linearly constrained minimum variance (LCMV) beamformer
361 approach was used (Gross, et al., 2001; Van Veen, Van Drongelen, Yuchtman, &
362 Suzuki, 1997), as implemented in Fieldtrip. Specifically, this source reconstruction
363 method scans every brain location testing for the likelihood of activity being on each of
364 them, based on the assumption that the time course at a given location is uncorrelated
365 with all other different sources. Importantly, the beamformer approach has several
366 advantages over the dipole modeling procedure, including no a priori assumptions about
367 the amount or the location of the underling sources. Thus, it implements an optimized
368 spatial filter that unifies two constraints: the maximization of the activity at the location
369 of interest and the suppression of all other interfering activity out of interest (i.e., noise
370 and other sources). The procedure followed two steps: forward and inverse model

computation. First, to ensure maximal specificity, a forward model derived from a standardized realistic head model was computed, defining how each source is visible at the scalp level. To this end, the volume conductor was discretized in a regular 3-D grid of 12 mm and the leadfield matrix was computed for each voxel. Then, a common spatial filter between stop and ignore conditions was designed. To this end, time segments of both experimental conditions were concatenated and re-referenced to the common average. Then the covariance matrix was calculated to determine the spatial filter coefficients. Thus, the source strength at each grid point was estimated by multiplying data for each experimental condition by this common filter. Based on the results of the statistical comparison between the time-frequency decompositions of stop and ignore trials at scalp level, data was bandpass filtered in the frequency range of interest. Then, the absolute value of its Hilbert transform was computed from -200 to +700 ms respect the go stimulus, separately for each experimental condition and individual subject. Once we identified which frequency band was sensitive to the experimental manipulation at the surface level, frequency resolution was no longer relevant for beamforming source reconstruction. Thus, we used the continuous Hilbert transform, rather than the short-time FFT, to better capture the time course of the effects. Before submitting source estimations to statistical analysis, a baseline transform was performed to control against the power bias towards the center of the head. Concretely, for each subject and experimental condition, absolute power changes with respect to baseline was calculated at each source grid location [(post-stimulus power − pre-stimulus power)].

2.4.5. Statistical analysis at source level

Cortical power volumes for the stop and ignore conditions were then submitted to statistical analysis. Oscillatory power projected into cortical source space for stop and ignore conditions was compared using the same nonparametric cluster-based permutation statistics as described for the time frequency scalp level data. However, as the beamformer solutions (3-dimensional dipole grids in MNI space) already reflect power changes within a certain time-frequency window, clusters were formed along the spatial dimension only.

3. Results

3.1. Behavioral results

As explained before, the strategy followed by each participant was estimated by comparing their mean no-signal (go) RT, stop-respond RT and ignore RT. The result of these analyses indicated that none of the subjects adopted an *iDtS* strategy to perform the task. Evidence for the use of the *StD* strategy was found in 33 out of the 54 subjects. Therefore, the remaining 21 subjects used a *dDtS* strategy. Repeated measures t-tests performed at group level corroborated this individual distinction. In the *StD* group, mean stop-respond RT were faster than mean no-signal RT ($t(32)=-8.591$, $p<0.001$, Cohen´s $d=1.78$), and mean ignore RT were slower than mean no-signal RT ($t(32) =-14.259$, $p<0.001$, Cohen´s $d=-2.21$). The group that adopted a *dDtS* strategy showed mean stop-respond RT no significantly slower than mean no-signal RT ($t(20)=-0.602$, $p=0.554$), and mean ignore RTs slower than mean no-signal RTs ($t(20)=-27.676$, $p<0.001$, Cohen´s $d=-4.253$). Their cumulative distributions are represented in Figure 2. Means and standard deviations RTs across strategies are shown in Table 1.

*** Table 1 around here***

*** Figure 2 around here***

SSRTs over both go and ignore distributions were computed for each strategy using the integration method (means and SD are shown in Table 1), knowing that this computation was only strictly valid for the *StD* strategy (Bissett & Logan, 2014).

3.2. Time-frequency results

Stop then Discriminate (StD) strategy

Figure 3a shows the grand-averaged time-frequency plot for each condition in a representative electrode. Significant clusters were observed above the significant threshold. However, differences were highly patent in the opposite direction, with higher power for ignore relative to successful stop condition (Figure 3c). Specifically, differences were observed between spectral changes induced by successful ignore relative to successful stop condition in theta and low-beta bands (ps<0.001). Regarding the former, the time course of statistical significance revealed that the effect only started after SSRT ending (after 380 ms), and was visible in the whole scalp (Figure 3c and Supplementary Figure 1a). Regarding the latter, ignore low-beta power started to be significantly more positive than stop related activity at 130 ms. and lasted until the end of the trial; however, differences were interrupted between 240 and 400 ms after signal presentation (just at the time of the SSRT and the ignore RT latency) in almost all electrode positions (Figure 3c and Supplementary Figure 1b). No differences were observed either in the high-beta (negative-cluster, p=0.27) or the gamma bands (negative-cluster, p=0.13). Given its latency, none of the differences observed at scalp

444 level could be related to response cancellation process. Therefore, source reconstruction
445 was not performed in this group of subjects.
446
447 *** Figure 3 around here***
448
449 *Dependent Discriminate then Stop (dDtS) strategy*
450 Figure 3b shows the grand-averaged time-frequency plot for each condition in a
451 representative electrode. When this strategy was used, the stop processing induced
452 significant increased high beta band activity relative to the ignore condition from 260 to
453 514 ms after the stop stimulus onset (cluster-based permutation test, p=0.021; Figure 3d
454 and Figure 4). Differences started at left frontal electrodes and then expanded to almost
455 all frontal and fronto-central locations (Figure 4ab). Notably, the estimated latency of
456 the end of the stop process (i.e., the SSRT) matched the timing of the differences
457 observed in the high beta-band between stop and ignore conditions in this strategy (see
458 vertical lines on x-axes in Figure 3d). No significant differences were observed in the
459 theta (negative-cluster, p=0.16) or in the gamma bands (negative-cluster, p=0.12).
460
461 *** Figure 4 around here***
462
463 To reconstruct the neural generators underlying high beta activation differences
464 between stop and ignore conditions, a beamforming analysis was performed at 21-30Hz
465 frequency range in a 50 ms time window around the estimated SSRT. Figure 4b shows
466 significant clusters ($p<0.05$) arising from a cluster-based permutation test (Maris &
467 Oostenveld, 2007). The main generator of these differences (stop>ignore) was located
468 in the anterior portion of the medial superior frontal cortex (pre-supplementary motor

area, preSMA; BAs 8; MNI coordinates X=-18, Y=29, Z=38; see Figure 5), extending to dorsolateral prefrontal regions (BA 9) and medially to anterior cingulate cortex (BA 32 and BA 24).

*** Figure 5 around here***

Ad hoc between-strategy analysis

The results of within-strategy analyses, both at the surface and voxel level, suggested that high-beta oscillations are critically involved in selective response cancellation. However, beta-band oscillations have also been implicated in motor response execution (Engel & Fries, 2010; Kilavik et al., 2013). Thus, in order to provide further support for the role of high-beta oscillations in selective response cancellation, we compared the ignore condition of the *dDtS* with the ignore condition of the *StD* strategy. We chose this comparison because ignore trials in the *StD* involve first response cancellation followed by response execution, whereas only response execution is need for ignore trials in the *dDtS* (in this strategy, individuals do not inhibit their responses in the ignore condition: (Bissett & Logan, 2014). Therefore, the results from this between-strategy analysis, might be particularly relevant to establish the role of high-beta activity in response cancellation. In particular, we expected higher high-beta activity for ignore *StD* than for *dDtS* ignore trials.

A cluster-based nonparametric permutation analysis was performed to compare ignore conditions between strategies using the same procedure as in the within-strategy analyses. We conducted one sided-test analyses in those time-channel samples showing higher high-beta power for *StD* ignore trials compared to *dDtS* ignore trials. The results revealed higher high-beta activity in *StD* ignore trials than in *dDtS* ignore trials (cluster-

based permutation test, p=0.04; Supplementary Figure 2). This increased activity emerged around the latency that has been estimated for the stop process in the *StD* (i.e., the SSRT: the time when the motor response is thought to be cancelled in this strategy). However, unlike the effect found in the successful stop versus ignore comparison within the *dDtS* strategy, the effect remained for several hundred milliseconds. This finding suggests that our between-strategy contrast involves additional processes beyond response cancellation. Therefore, although the results from the comparison between ignore trials in both strategies support the role of high beta band in response cancelation, some caution is needed when interpreting this ad hoc and little examined comparison.

4. Discussion

We investigated for the first time the oscillatory neuronal mechanisms supporting response cancellation for the two main strategies used in stimulus-selective stopping paradigms. Recent proposals have claimed that brain oscillations may play a central role in stopping, at least in a broad sense. Specifically, it has been argued that the frontosubthalamic circuit supporting global stopping might operate via communication trough the beta frequency band (Aron, et al., 2016). Although this proposal still needs further support, some evidence from electrophysiological studies points to a role of spectral changes in the beta band frequency range in response cancellation (Lavallee, et al., 2014; Pastötter, Hanslmayr, & Bäuml, 2008; N. Swann, et al., 2009; Wagner, et al., 2018). However, the mechanisms behind these effects remain to be clarified. Additionally, theta-band frequency oscillations have also been associated with stopping initiated responses (Isabella, et al., 2015; Jha, et al., 2015; Nigbur, et al., 2011), although it is still under debate whether theta-band effects are directly involved in

519 response cancellation or rather reflect a general marker of executive control or conflict
520 monitoring (Nigbur, et al., 2011). As we will elaborate later, here we provide support
521 for the view that oscillatory activity in the high beta frequency range, but not in the
522 theta band, is specifically associated with response cancellation.

523 Following the criteria proposed by Bisset and Logan (2014), we first identified
524 the strategy adopted by each participant to perform the stimulus-selective stop-signal
525 task. Most of them used the *StD* strategy (61%), which is characterized by stopping
526 non-selectively to both ignore and stop signals. The remaining participants (39%) used
527 the *dDtS* strategy in which the ongoing response is selectively interrupted when the stop
528 signal is presented. These percentages are similar to those observed in our previous
529 study (Sánchez-Carmona, et al., 2016), but differ from those reported by Bisset and
530 Logan (2014) and by Sebastian and colleagues (2017). One possible explanation for this
531 discrepancy is that these two studies used color as the feature to discriminate between
532 stop and ignore stimuli. By contrast, as in our prior study, we used here perceptually
533 similar geometric, black-colored shapes that only differed in orientation. Therefore, the
534 perceptual similarity between stop and ignore signals in our task might have biased
535 participants to adopt a more conservative strategy (i.e., *StD*). Indeed, the results from a
536 recent behavioral experiment supported this notion by showing that the degree of
537 perceptual similarity of ignore and stop signals bias strategy adoption processes
538 (Sánchez-Carmona et al., in preparation).

539 Subsequently, we examined oscillatory activation associated with response
540 cancellation for each strategy. We compared successful stop versus successful ignore
541 conditions, a comparison that has been recommended to identify the neural correlates
542 specifically linked to response cancellation (Etchell, et al., 2012; Sánchez-Carmona, et
543 al., 2016; Sharp, et al., 2010). This functional comparison seems to overcome some of

the limitations of traditional contrasts (e.g., successful stop vs. go, successful stop vs. failed stop) by minimizing the influence of confounding factors such as novelty, emotional and/or perceptive/sensory effects.

When comparing activity elicited by the successful stop and the ignore conditions in the selective stopping strategy (*dDtS*), we found increased power in the higher beta band. This effect seems to be related to a smaller high-beta band desynchronization for the stop relative to the ignore condition, which is in line with the results from several previous studies with non-selective stop signal and go/no go tasks that found reduced beta band desynchronization in response to stop/nogo trials (Kühn, et al., 2004; Nigbur, et al., 2011). It has been proposed that beta event-related desynchronization would represent active stopping mediated by a cortical inhibition, whereas beta event-related synchronization would reflect a decrease of cortical activation in a more passive way (Pastötter, et al., 2008). Notably, the increased activity in the high-beta frequency band during response cancellation in the *dDtS* strategy was more evident at frontal scalp electrodes and emerged just before the latency of the response cancellation process as measured by the SSRT computed over the ignore distribution (Bissett & Logan, 2014). Therefore, these results suggest that oscillatory activity in the high-beta frequency range is critically involved in response cancellation, extending the findings from a prior ERP investigation that observed differences between successful stop and successful ignore conditions at the onset of the P3 only in this strategy (Sánchez-Carmona, et al., 2016).

The comparison between successful stop and ignore conditions in the *dDtS* strategy was significant for the beta, but not for the theta band. Thus, we failed to provide evidence for the hypothesis that theta-band oscillatory activity specifically reflects the processing stage of response cancellation. Rather, it might represent a more

general marker of executive control, since we observed an increased theta-band activation for both stop and ignore relative to go stimulus (data not shown). This idea would be in line with some prior findings (Aron, et al., 2016; Cavanagh & Frank, 2014; Nigbur, et al., 2011). In a similar vein, no significant differences were observed in gamma activity, which suggests that this band is not specifically involved in selective response cancellation.

In the non-selective stopping strategy (*StD*), no stopping-related differences between successful stop and ignore conditions were observed in the high beta frequency band. Although null findings should be interpreted with caution, these results would suggest that both conditions induced equivalent spectral changes. Nonetheless, the absence of oscillatory activity differences between successful stop and ignore conditions at the time by which stopping process ended (SSRT) was an expected finding for the *StD* strategy. Indeed, prior behavioral data have shown that individuals who use this strategy stop their responses whenever a signal occurs without further discriminating between stop and ignore trials (Bisset & Logan, 2014). It has been suggested that spectral changes that are not specifically linked to response cancellation might underlay differences between the stop and ignore conditions within this strategy (Sebastian, et al., 2017). In accordance with this view, in the current experiment we observed differences in the *StD* strategy between successful stop and ignore trials in both the theta and low-beta bands. However, these differences were not in the expected direction since we found higher activity for ignore than for stop trials (reduced event-related desynchronization). It is worthy to mention that the latency of these effects makes it unlikely that they reflect response cancellation. On the one hand, differences in the theta band only started after SSRT ending, which could be associated with the higher conflict induced by the requirement of restarting a response for ignore condition in this strategy.

On the other hand, differences in the low-beta frequency band were vanished in the time range of both RTs and SSRT for ignored trials computed over the go distribution. It could be argued that this finding would reflect response cancellation in both conditions. However, to establish a reliable link between low-beta activity and response cancellation, similar modulations in this frequency band should have also been also observed in the *dDtS* strategy. Since we did not found such differences, we concluded that low beta oscillations do not seem to be related to selective stopping.

Regarding the neural origin of these effects, we found that the main cortical generator underlying differences in the high beta band between stop and ignore conditions in the *dDtS* strategy were mainly located in the medial superior frontal cortex, including the preSMA. This region, in conjunction with the IFC, is thought to play a key role in global stopping by implementing inhibitory control via direct inputs to the STN (the so-called *hyperdirect pathway*). Although the contribution of this brain area to selective stopping remains poorly understood, it has been hypothesized that reactive selective stopping may implemented via the so-called *indirect pathway* (Aron, 2011). Again, the preSMA (and/or the IFC) would be a critical region within this pathway that would involve the additional activation of the caudate and the external globus pallidus (see Figure 5 of Aron, 2011). Here, we provide further evidence for this hypothesis by showing a critical involvement of the preSMA in response cancellation during selective stopping. Additionally, we found activation of the dorsolateral prefrontal cortex (dlPFC) during response cancellation in the *dDtS* strategy. Although the dlPFC is not typically activated in global stopping tasks, some authors have suggested that this region could be involved in other complex forms of inhibition (including proactive and selective stopping), in which working memory and decision-making demands increase (Aron, 2011; Smittenaar, Guitart-Masip, Lutti, & Dolan,

2013). Indeed, higher activation of the dlPFC for the stop relative to the ignore condition in the *dDts* strategy was also observed in a previous stimulus-selective stopping study using ERP in conjunction with LORETA source reconstruction procedures (Sánchez-Carmona, et al., 2016).

It should also be noted that stopping-related activation was primarily observed in left-lateralized cortical regions. Although global stopping typically involved a right-hemisphere network, bilateral and left-lateralized activation has also been reported (Albert, et al., 2013; Hirose, et al., 2012; Li, et al., 2006; Swick, Ashley, & Turken, 2008; Zhang & Li, 2012). We speculate that discriminating between stop and ignore signals before the suppression of the response in selective stop-signal tasks could induce a more serial form of processing compared to non-selective stop-signal tasks, which do not involve such discrimination. This serial processing would trigger resetting operations in working memory linked to the activation of brain structures in the left rather than in right frontal cortices.

Although the successful stop versus ignore comparison seems to overcome some of the limitations of traditional contrasts, the contribution of motor response effects could not be totally ruled out since stop - but not ignore - trials involve motor response execution. Thus, it would be possible that the high-beta effect observed in the *dDtS* strategy may reflect motor preparation or response execution instead of selective stopping. Indeed, beta oscillations are strongly believed to be implicated in motor response execution (Engel & Fries, 2010; Kilavik, Zaepffel, Brovelli, MacKay, & Riehle, 2013). However, there are several reasons that suggest that the increased activation in the beta band observed here could be primarily linked to response cancellation. First, differences between the successful stop and ignore conditions in the selective response cancellation group (*dDtS*) were only found in the high-beta frequency

band, and only near the end of the SSRT (i.e., just at the time when the motor response is estimated to be cancelled in this strategy). Second, as expected, no differences were observed in the high-beta band between the successful stop and ignore conditions in the *StD* group, where response cancellation is thought to be non-selectively activated in both conditions (Bisset & Logan, 2014). Third, the increased high beta band activity observed in the *dDtS* group was estimated to arise from regions typically associated with stopping (the preSMA) rather than with responding.

Nevertheless, in order to get further evidence for the involvement of high-beta band in response cancellation, we performed an ad hoc analysis comparing activity in the ignore condition in the *StD* and the *dDtS* strategies. Of note, ignore trials in the *StD* strategy involve firstly response cancellation and subsequently response execution, whereas ignore trials in the *dDtS* only involve response execution (in this strategy, individuals do not inhibit their responses within this condition: (Bissett & Logan, 2014). As expected, we found greater activity in the high-beta band in the *StD* than in the *dDtS* strategy. This increased activity emerged at the end of the SSRT in the *StD* (i.e., just at the time when the motor response is thought to be cancelled in this strategy). Remarkably, unlike results reported in the stop versus ignore comparison in the *dDtS* strategy, these effects lasted for several hundred milliseconds, indicating that the comparison between ignore trials in both strategies involves additional processes beyond response cancellation. Thus, although these data also argues for a role of high-beta activity in response cancelation, some caution is needed when interpreting this scarcely explored functional comparison.

In summary, present results contribute to our understanding of the neural mechanisms underlying selective stopping strategies. We found that a successful cancelation of an initiated response is specifically associated with an increased

oscillatory activity in the high-beta frequency band in the strategy characterized by stopping selectively (*dDtS*), but not in the strategy characterized by stopping non-selectively (*StD*). These findings provide further neural support for the existence of different strategies for successfully performing stimulus-selective stopping tasks (Bissett & Logan, 2014; Sánchez-Carmona, et al., 2016; Sebastian, et al., 2017). Moreover, they provide evidence suggesting that high-beta oscillations in medial superior and middle frontal cortices may constitute an important neural marker of response cancellation.

Acknowledgements: This work was supported by grants PSI2015-68368-P and PSI2017-84922-R (MINECO), and H2015/HUM-3327 from the Comunidad de Madrid. The authors thank Frederick Verbruggen for providing us the Matlab script of STOP-IT.

Conflict of interest: The authors declare no competing financial interests.

References

Albert, J., López-Martín, S., Hinojosa, J. A., & Carretié, L. (2013). Spatiotemporal characterization of response inhibition. *Neuroimage, 76*, 272-281.

Aron, A. R. (2011). From reactive to proactive and selective control: developing a richer model for stopping inappropriate responses. *Biological psychiatry, 69*, e55-e68.

Aron, A. R., Herz, D. M., Brown, P., Forstmann, B. U., & Zaghloul, K. (2016). Frontosubthalamic circuits for control of action and cognition. *Journal of Neuroscience, 36*, 11489-11495.

Bissett, P. G., & Logan, G. D. (2014). Selective stopping? Maybe not. *Journal of Experimental Psychology: General, 143*, 455.

Cavanagh, J. F., & Frank, M. J. (2014). Frontal theta as a mechanism for cognitive control. *Trends in cognitive sciences, 18*, 414-421.

Cohen, M. X. (2014). *Analyzing neural time series data: theory and practice*. Cambridge, USA: MIT press.

Chikazoe, J., Konishi, S., Asari, T., Jimura, K., & Miyashita, Y. (2007). Activation of right inferior frontal gyrus during response inhibition across response modalities. *Journal of Cognitive Neuroscience, 19*, 69-80.

Engel, A. K., & Fries, P. (2010). Beta-band oscillations—signalling the status quo? *Current opinion in neurobiology, 20*, 156-165.

Etchell, A. C., Sowman, P. F., & Johnson, B. W. (2012). "Shut up!" An electrophysiological study investigating the neural correlates of vocal inhibition. *Neuropsychologia, 50*, 129-138.

Faul, F., Erdfelder, E., Buchner, A., & Lang, A.-G. (2009). Statistical power analyses using G* Power 3.1: Tests for correlation and regression analyses. *Behavior research methods, 41*, 1149-1160.

Gross, J., Kujala, J., Hämäläinen, M., Timmermann, L., Schnitzler, A., & Salmelin, R. (2001). Dynamic imaging of coherent sources: studying neural interactions in the human brain. *Proceedings of the National Academy of Sciences, 98*, 694-699.

Hirose, S., Chikazoe, J., Watanabe, T., Jimura, K., Kunimatsu, A., Abe, O., Ohtomo, K., Miyashita, Y., & Konishi, S. (2012). Efficiency of go/no-go task performance implemented in the left hemisphere. *Journal of Neuroscience, 32*, 9059-9065.

Huster, R. J., Enriquez-Geppert, S., Lavallee, C. F., Falkenstein, M., & Herrmann, C. S. (2013). Electroencephalography of response inhibition tasks: functional networks and cognitive contributions. *International Journal of Psychophysiology, 87*, 217-233.

Isabella, S., Ferrari, P., Jobst, C., Cheyne, J. A., & Cheyne, D. (2015). Complementary roles of cortical oscillations in automatic and controlled processing during rapid serial tasks. *Neuroimage, 118*, 268-281.

Jha, A., Nachev, P., Barnes, G., Husain, M., Brown, P., & Litvak, V. (2015). The frontal control of stopping. *Cerebral Cortex, 25*, 4392-4406.

Jung, T.-P., Makeig, S., Humphries, C., Lee, T.-W., Mckeown, M. J., Iragui, V., & Sejnowski, T. J. (2000). Removing electroencephalographic artifacts by blind source separation. *Psychophysiology, 37*, 163-178.

Kilavik, B. E., Zaepffel, M., Brovelli, A., MacKay, W. A., & Riehle, A. (2013). The ups and downs of beta oscillations in sensorimotor cortex. *Experimental neurology, 245*, 15-26.

Kühn, A. A., Williams, D., Kupsch, A., Limousin, P., Hariz, M., Schneider, G. H., Yarrow, K., & Brown, P. (2004). Event-related beta desynchronization in human subthalamic nucleus correlates with motor performance. *Brain, 127*, 735-746.

Lavallee, C. F., Meemken, M. T., Herrmann, C. S., & Huster, R. J. (2014). When holding your horses meets the deer in the headlights: time-frequency characteristics of global and selective stopping under conditions of proactive and reactive control. *Frontiers in human neuroscience, 8*, 994.

Levitt, H. (1971). Transformed up-down methods in psychoacoustics. *The Journal of the Acoustical society of America, 49*, 467-477.

Li, C.-s. R., Huang, C., Constable, R. T., & Sinha, R. (2006). Imaging response inhibition in a stop-signal task: neural correlates independent of signal monitoring and post-response processing. *Journal of Neuroscience, 26*, 186-192.

Li, C.-s. R., Yan, P., Sinha, R., & Lee, T.-W. (2008). Subcortical processes of motor response inhibition during a stop signal task. *Neuroimage, 41*, 1352-1363.

Logan, G. D. (1994). On the ability to inhibit thought and action: A users' guide to the stop signal paradigm.

Marco-Pallarés, J., Camara, E., Münte, T. F., & Rodríguez-Fornells, A. (2008). Neural mechanisms underlying adaptive actions after slips. *Journal of Cognitive Neuroscience, 20*, 1595-1610.

Maris, E., & Oostenveld, R. (2007). Nonparametric statistical testing of EEG-and MEG-data. *Journal of neuroscience methods, 164*, 177-190.

Nigbur, R., Ivanova, G., & Stürmer, B. (2011). Theta power as a marker for cognitive interference. *Clinical Neurophysiology, 122*, 2185-2194.

Oostenveld, R., Fries, P., Maris, E., & Schoffelen, J.-M. (2011). FieldTrip: open source software for advanced analysis of MEG, EEG, and invasive electrophysiological data. *Computational intelligence and neuroscience, 2011*, 1.

Pastötter, B., Hanslmayr, S., & Bäuml, K.-H. (2008). Inhibition of return arises from inhibition of response processes: an analysis of oscillatory beta activity. *Journal of Cognitive Neuroscience, 20*, 65-75.

Ritter, P., Moosmann, M., & Villringer, A. (2009). Rolandic alpha and beta EEG rhythms' strengths are inversely related to fMRI-BOLD signal in primary somatosensory and motor cortex. *Human brain mapping, 30*, 1168-1187.

Rouder, J. N., Speckman, P. L., Sun, D., Morey, R. D., & Iverson, G. (2009). Bayesian t tests for accepting and rejecting the null hypothesis. *Psychonomic bulletin & review, 16*, 225-237.

Sánchez-Carmona, A. J., Albert, J., & Hinojosa, J. A. (2016). Neural and behavioral correlates of selective stopping: evidence for a different strategy adoption. *Neuroimage, 139*, 279-293.

Sebastian, A., Rößler, K., Wibral, M., Mobascher, A., Lieb, K., Jung, P., & Tüscher, O. (2017). Neural architecture of selective stopping strategies—distinct brain activity patterns are associated with attentional capture but not with outright stopping. *Journal of Neuroscience*, 1476-1417.

Sharp, D., Bonnelle, V., De Boissezon, X., Beckmann, C., James, S., Patel, M., & Mehta, M. A. (2010). Distinct frontal systems for response inhibition, attentional capture, and error processing. *Proceedings of the National Academy of Sciences, 107*, 6106-6111.

Smittenaar, P., Guitart-Masip, M., Lutti, A., & Dolan, R. J. (2013). Preparing for selective inhibition within frontostriatal loops. *Journal of Neuroscience, 33*, 18087-18097.

Swann, N., Tandon, N., Canolty, R., Ellmore, T. M., McEvoy, L. K., Dreyer, S., DiSano, M., & Aron, A. R. (2009). Intracranial EEG reveals a time-and frequency-specific role for the right inferior frontal gyrus and primary motor cortex in stopping initiated responses. *Journal of Neuroscience, 29*, 12675-12685.

Swann, N. C., Cai, W., Conner, C. R., Pieters, T. A., Claffey, M. P., George, J. S., Aron, A. R., & Tandon, N. (2012). Roles for the pre-supplementary motor area and the right inferior frontal gyrus in stopping action: electrophysiological responses and functional and structural connectivity. *Neuroimage, 59*, 2860-2870.

Swick, D., Ashley, V., & Turken, U. (2008). Left inferior frontal gyrus is critical for response inhibition. *BMC neuroscience, 9*, 102.

Van Veen, B. D., Van Drongelen, W., Yuchtman, M., & Suzuki, A. (1997). Localization of brain electrical activity via linearly constrained minimum variance spatial filtering. *IEEE Transactions on biomedical engineering, 44*, 867-880.

Verbruggen, F., Chambers, C. D., & Logan, G. D. (2013). Fictitious inhibitory differences: how skewness and slowing distort the estimation of stopping latencies. *Psychological science, 24*, 352-362.

Verbruggen, F., & Logan, G. D. (2009). Models of response inhibition in the stop-signal and stop-change paradigms. *Neuroscience & Biobehavioral Reviews, 33*, 647-661.

Verbruggen, F., Logan, G. D., & Stevens, M. A. (2008). STOP-IT: Windows executable software for the stop-signal paradigm. *Behavior research methods, 40*, 479-483.

Wagner, J., Wessel, J. R., Ghahremani, A., & Aron, A. R. (2018). Establishing a right frontal beta signature for stopping action in scalp EEG: implications for testing inhibitory control in other task contexts. *Journal of Cognitive Neuroscience, 30*, 107-118.

Wessel, J. R., & Aron, A. R. (2014). Inhibitory motor control based on complex stopping goals relies on the same brain network as simple stopping. *Neuroimage, 103*, 225-234.

Zhang, S., & Li, C. s. R. (2012). Functional networks for cognitive control in a stop signal task: independent component analysis. *Human brain mapping, 33*, 89-104.

Figure 1. Schematic representation of the stimulus-selective stop signal task.

Figure 2. Quantile averages of RT for stop-respond trials, no-signal (Go) trials, and ignore trials for participants who adopted the *Stop then Discriminate* (*StD*) strategy (a), and subjects who adopted the dependent *Discriminate then Stop* (*dDtS*) strategy (b).

Figure 3. Time-frequency plots for the successful stop and successful ignore conditions in the *Stop then Discriminate* (*StD*) strategy (a) and *dependent Discriminate then Stop* (dDtS) strategy (b) for 2.5 to 50 Hz at a representative electrode location (FC3). To avoid artifact contamination, a -400 to -200 baseline prior go stimulus onset was used. Thus, x-axis was broken in two sections, to show both pre-go baseline and signal-related power. Total power is expressed as decibel transformation relative to baseline. The dotted vertical line indicates the signal onset (ignore or stop). Time-frequency plot for the power difference between successful stop and successful ignore trials in the *StD* (c) and *dDts* (d) strategy. Relative power was averaged over the significant electrodes observed in statistical analyses. The black box highlights both the frequencies and the time ranges in which significant results were observed.in each strategy. The black vertical line on the x-axis represents the mean stop signal reaction time (SSRT) for each strategy.

Figure 4. a) Topographic distribution along the time course of the significant cluster observed in the high-beta frequency band (21-30 Hz) between successful stop and successful ignore trials in the *dependent Discriminate then Stop* (*dDtS)* strategy. Significant electrodes ($p<0.02$) are highlighted with a black star. Color bar represents t values. b) Positive significant clusters of non-parametrical permutation analysis in the high-beta frequency band showing greater power for successful stop compared to successful ignore condition in the *dDtS* strategy. Color bar represents t values. c) Time course of total high-beta power, averaged for significant electrodes, comparing successful stop and successful ignore trials in the *dDtS* strategy. Dashed lines represent 95% confidence interval.

Figure 5. Beamforming reconstruction of the neural sources of high-beta band activity observed at the scalp level in the *dependent Discriminate then Stop (dDtS)* strategy (successful stop > successful ignore). Color bar represents t values

Supplementary Figure 1. a) Negative significant clusters of non-parametrical permutation analysis in theta (a) and low-beta (b) frequency bands for the successful stop versus successful ignore comparison in the *Stop then Discriminate (StD)* strategy (i.e., greater power for successful ignore compared to successful stop condition was found). Color bar represents t values.

Supplementary Figure 2. a) Positive significant clusters of non-parametrical permutation analysis in high-beta frequency band (21-30 Hz) showing greater power for successful ignore trials in the *Stop then Discriminate* (StD) strategy compared to successful ignore trials in the *dependent Discriminate then Stop (dDtS)* strategy. Color bar represents t values. b) Time course of total high-beta power, averaged for significant electrodes, comparing ignore conditions between strategies. Dashed lines represent 95% confidence interval.

Table 1. Sample characteristics and task performance of study participants (means and standard deviations).

	dDtS	StD
N	21	33
Age	21.14 (1.45)	20.75 (1.39)
No-signal	436.58 (25.19)	547.09 (44.68)
Stop	433.87 (20.86)	488.95 (10.98)
Ignore	523.01 (13.81)	625.30 (22.12)
SSRT go	291.31 (57.54)	246.83(57.34)
SSRT ignore	378.84 (51.05)	307.24 (69.60)
Mean SSD	169.93 (30.92)	308.33(80.24)

Abbreviations: dDtS, dependent Discriminate then Stop strategy; StD, Stop then Discriminate strategy; RT, reaction times; SSRT, stop signal reaction times; SSRTgo, SSRT computed on the go distribution using the integration method; SSRTignore, SSRT computed on the ignore distribution using the integration method. Mean SSD, mean stop signal delay.

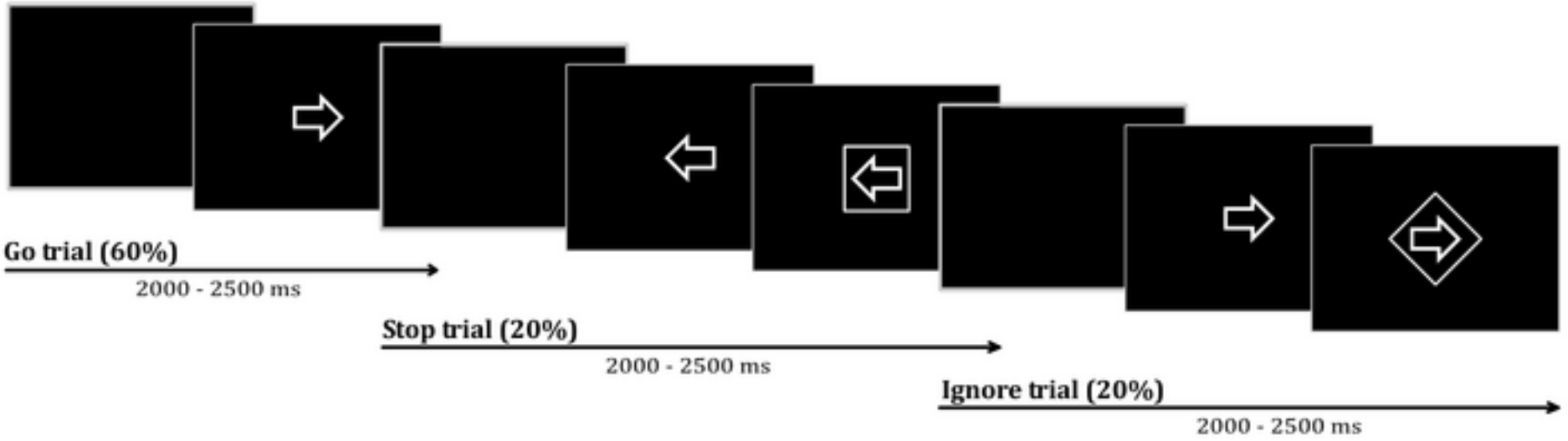
Go trial (60%)
2000 - 2500 ms
Stop trial (20%)
2000 - 2500 ms
Ignore trial (20%)
2000 - 2500 ms

a)

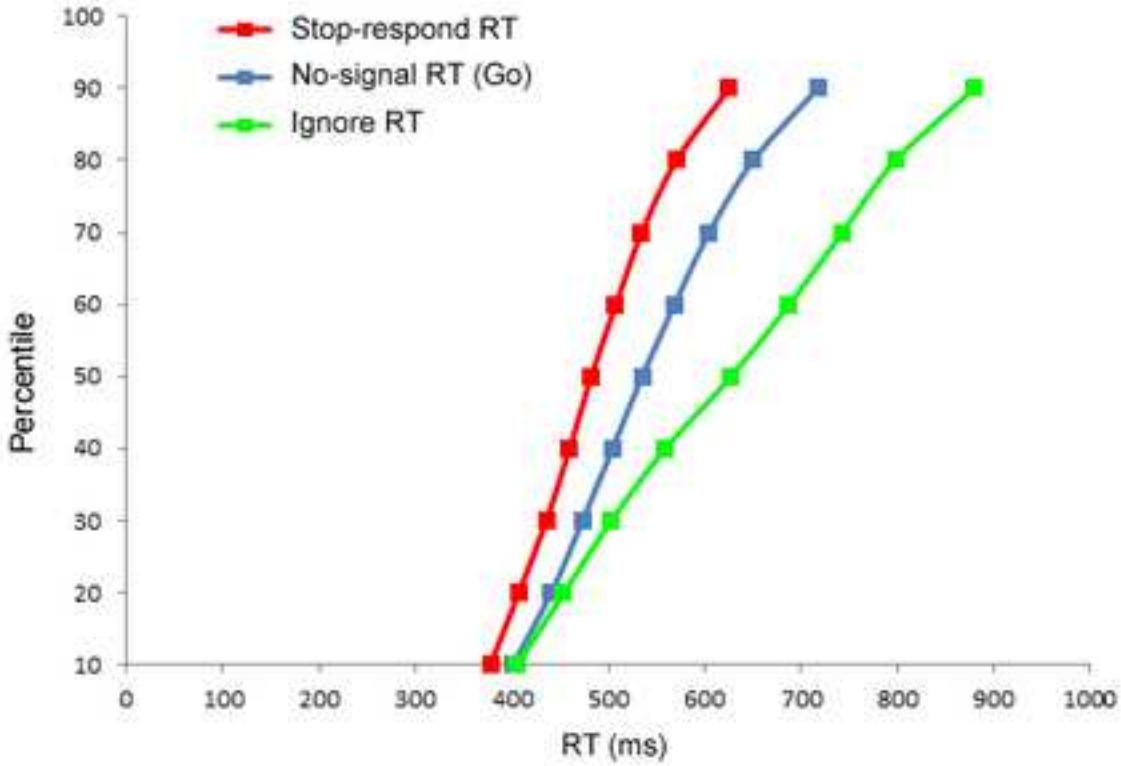
Stop-respond RT
No-signal RT (Go)
Ignore RT
Percentile
RT (ms)
100
90
80
70
60
50
40
30
20
10
0
100
200
300
400
500
600
700
800
900
1000

b)

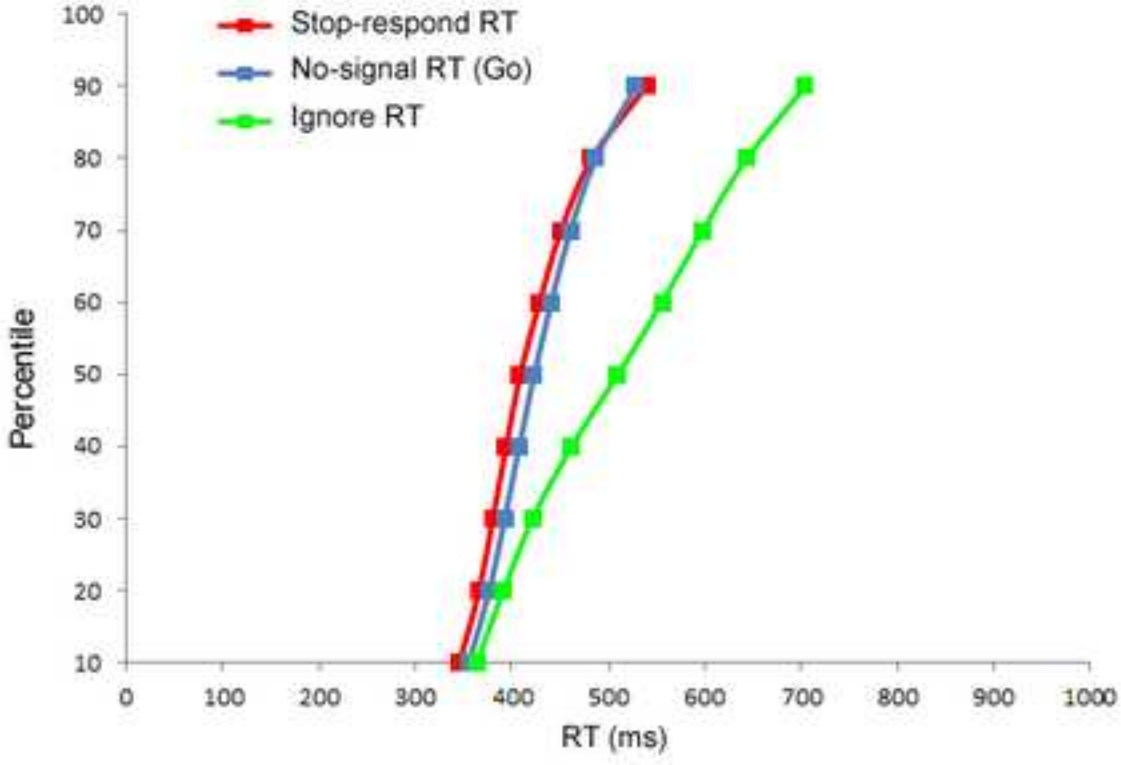
Stop-respond RT
No-signal RT (Go)
Ignore RT
Percentile
RT (ms)
100
90
80
70
60
50
40
30
20
10
0
100
200
300
400
500
600
700
800
900
1000

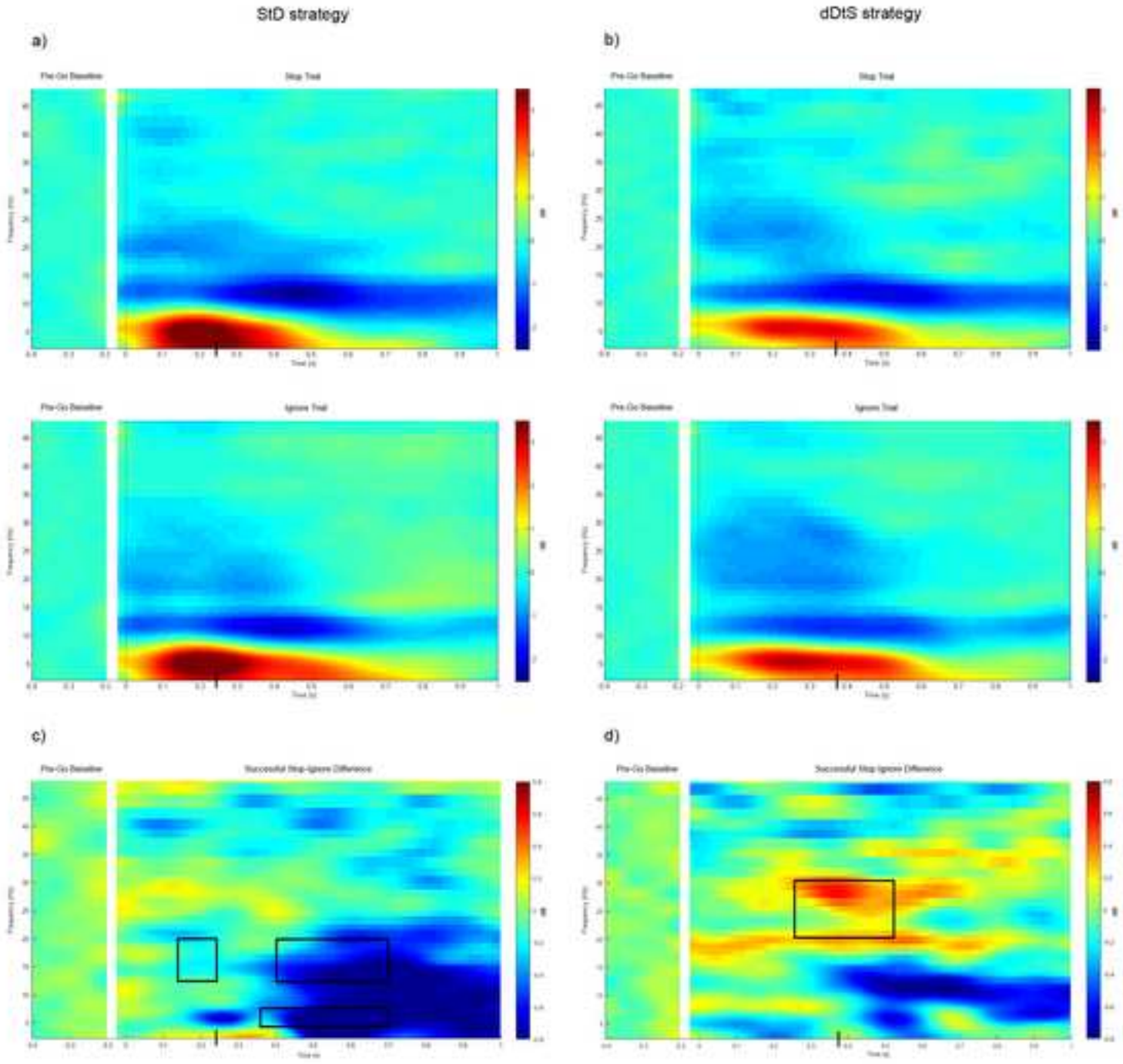
StD strategy
dDtS strategy
a)
b)
c)
d)

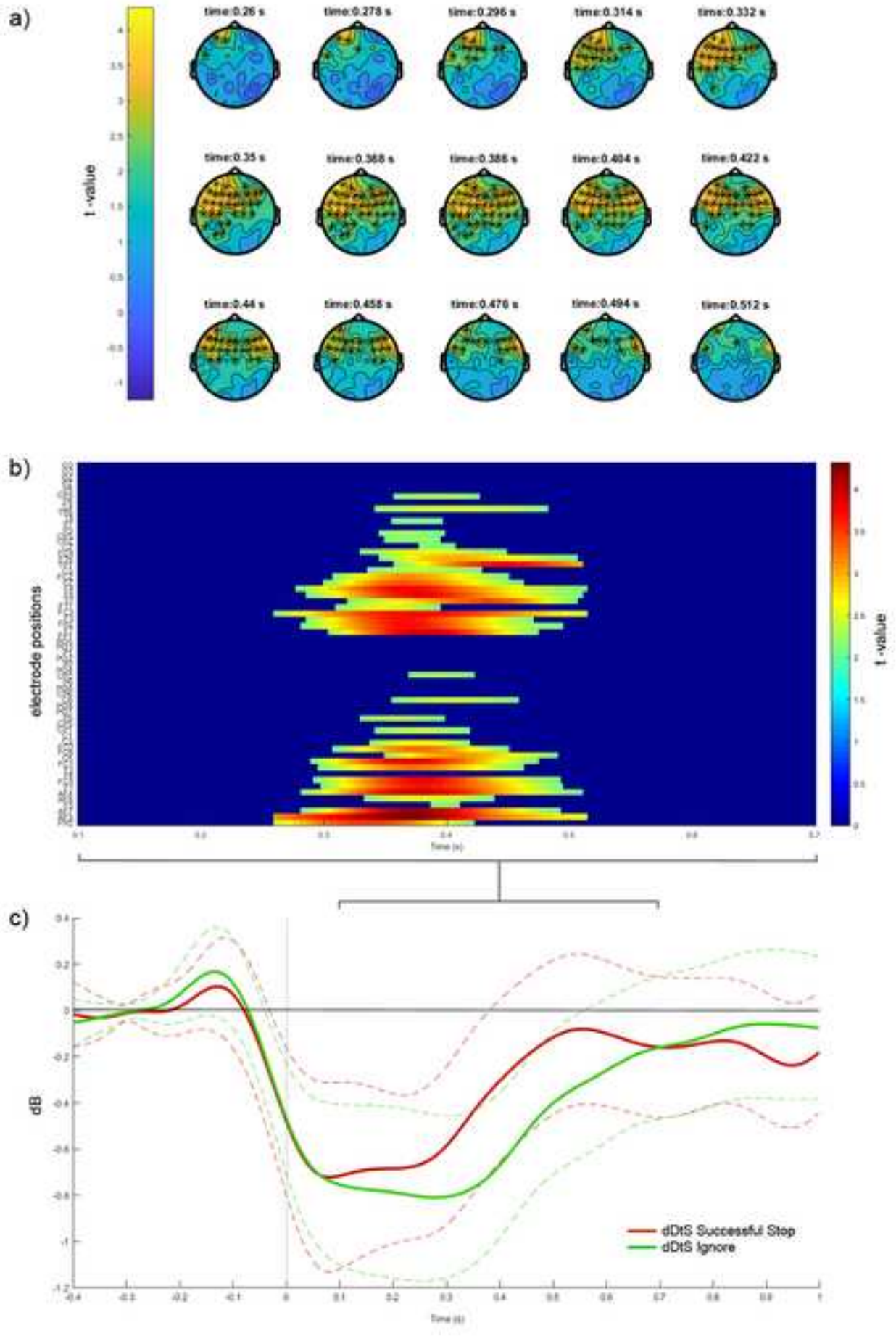
a)
t -value
time:0.26 s
time:0.278 s
time:0.296 s
time:0.314 s
time:0.332 s
time:0.35 s
time:0.368 s
time:0.386 s
time:0.404 s
time:0.422 s
time:0.44 s
time:0.458 s
time:0.476 s
time:0.494 s
time:0.512 s
b)
electrode positions
t -value
Time (s)
c)
dB
dDtS Successful Stop
dDtS Ignore
Time (s)

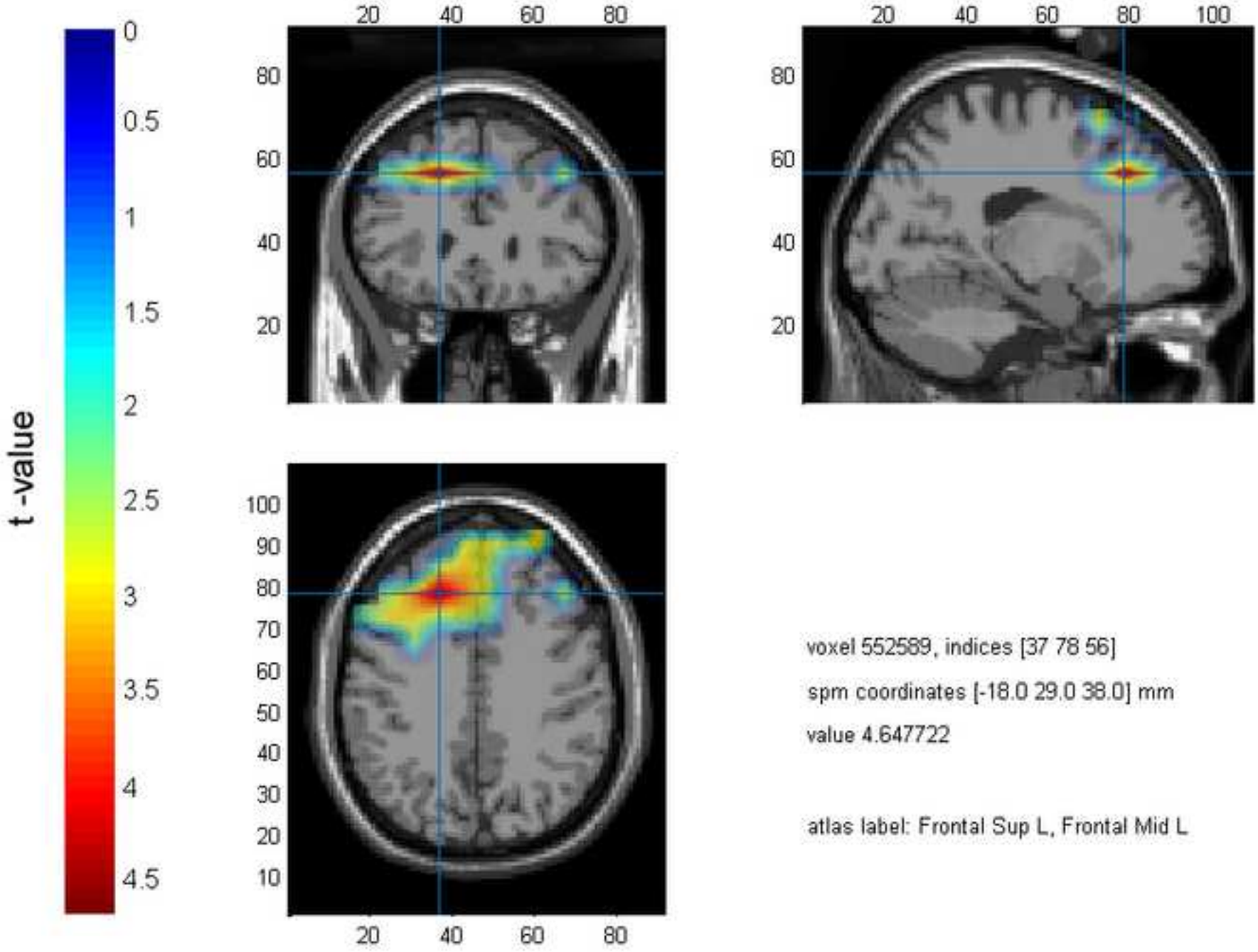
t -value
0
0.5
1
1.5
2
2.5
3
3.5
4
4.5
20
40
60
80
100
10
30
50
70
90
voxel 552589, indices [37 78 56]
spm coordinates [-18.0 29.0 38.0] mm
value 4.647722
atlas label: Frontal Sup L, Frontal Mid L

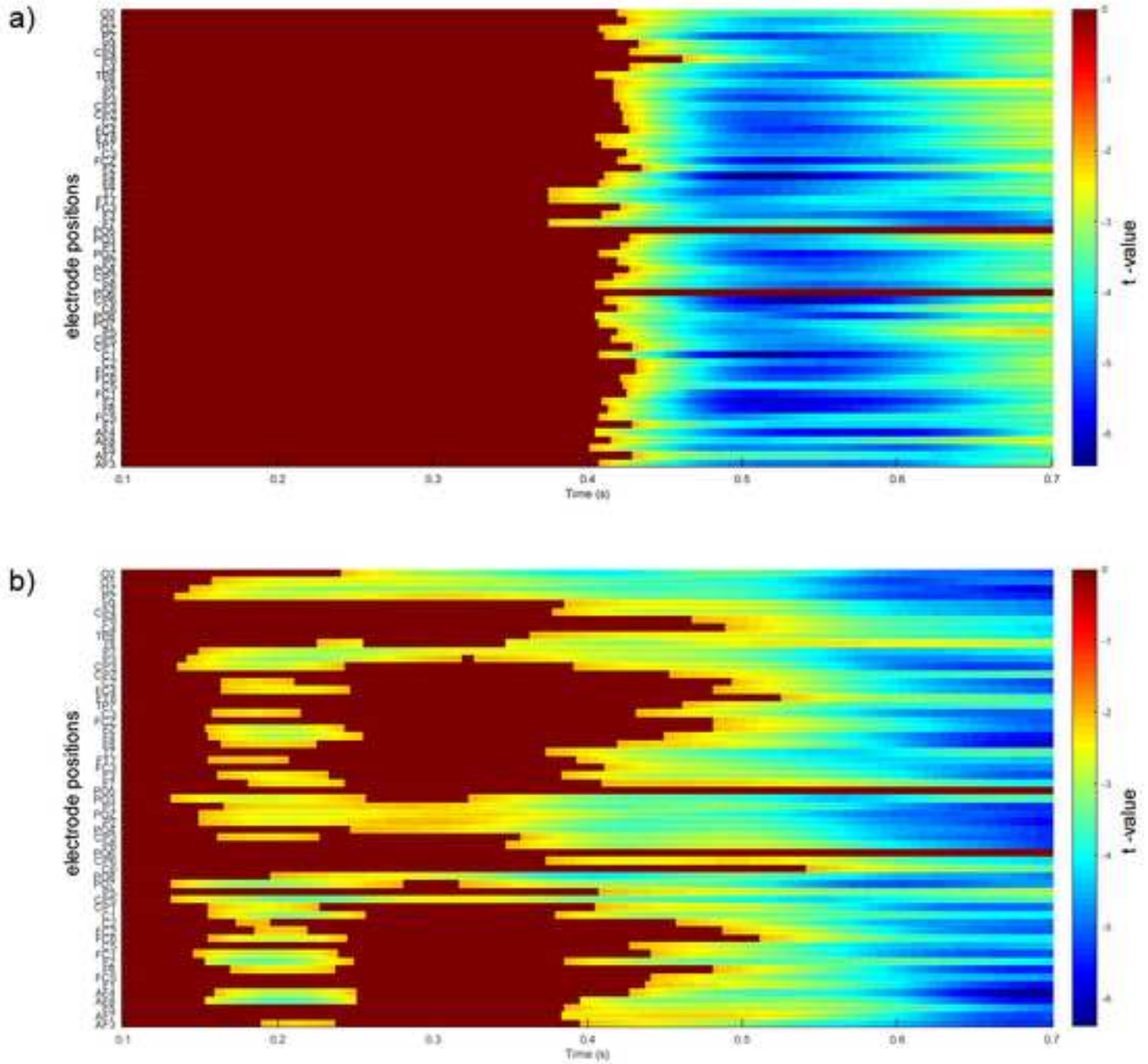
a)
b)
electrode positions
Time (s)
t -value

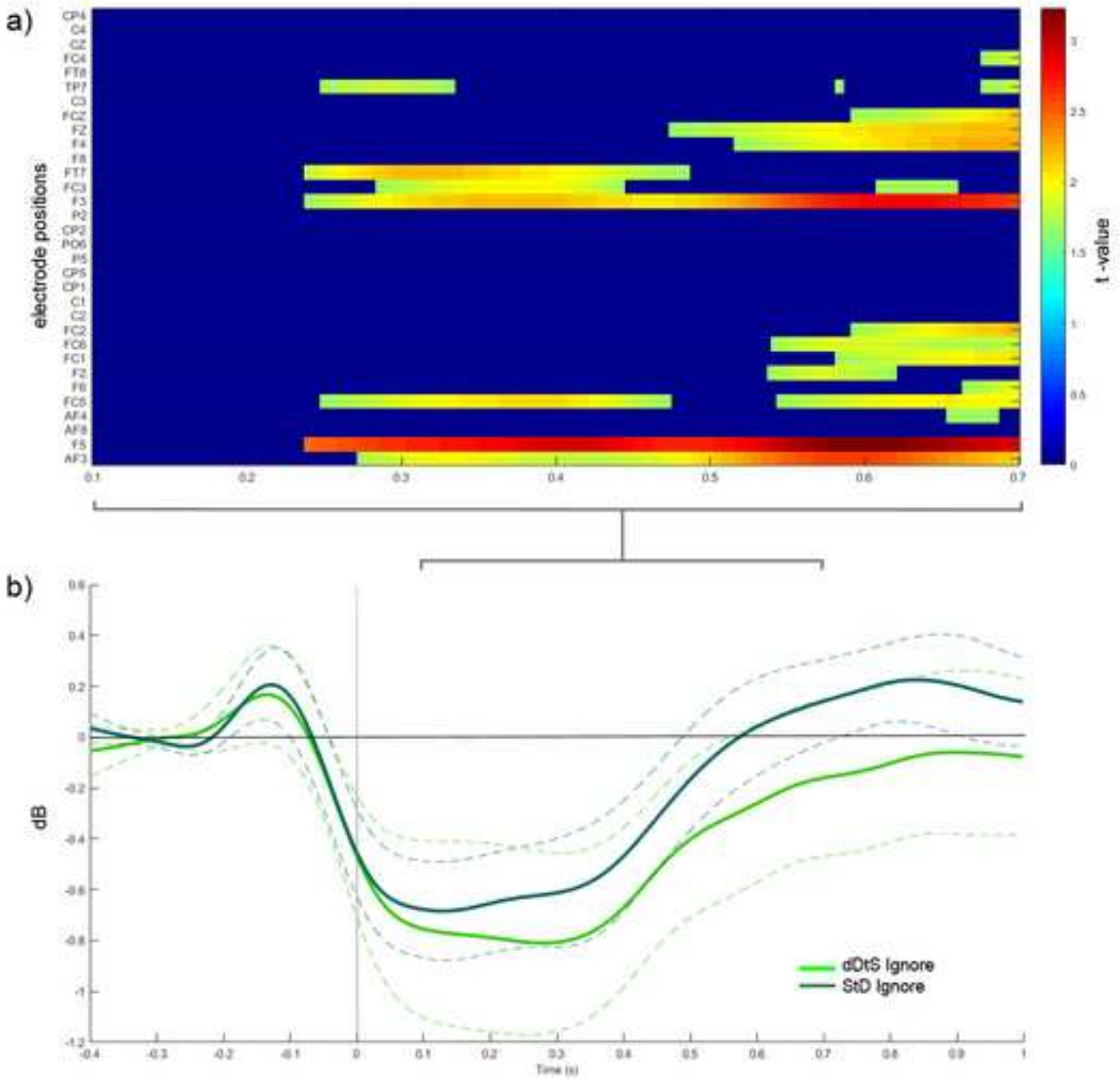
a)
electrode positions
CP4
C4
CZ
FC4
FT8
TP7
C3
FCZ
FZ
F4
F8
FT7
FC3
F3
P2
CP2
PO6
P5
CP5
CP1
C1
C2
FC2
FC6
FC1
FZ
F6
FC5
AF4
AF8
F5
AF3
0.1
0.2
0.3
0.4
0.5
0.6
0.7
t -value
b)
dB
Time (s)
dDtS Ignore
StD Ignore